Optimal Elasto-Plastic Analysis of Reinforced Concrete Structures under Residual Plastic Deformation Limitations

Sarah Khaleel Ibrahim, Majid Movahedi Rad*, Szabolcs Fischer

Széchenyi István University, Egyetem tér 1, 9026 Győr, Hungary
e-mail: sarah.khaleel.ibrahim@hallgato.sze.hu; majidmr@sze.hu; fischersz@sze.hu

Abstract: In this study, an investigation regarding optimal elastic-plastic analysis method of different reinforced concrete (RC) structures is held by applying the residual plastic deformations limitations on the steel bars inside the reinforced concrete. Where different structures, including simple beam and slab, are selected as benchmarks and modelled numerically using ABAQUS in order to calibrate their experimental behaviour according to laboratory tests. Furthermore, concrete damage plasticity (CDP) constitutive model was applied to represent concrete behaviour in the numerical models considered. Then, an objective function was established for optimizing the applied plastic loads for each structure where the process of controlling plastic deformations was carried out by applying constraints on the complementary strain energy of the residual internal forces initiated inside the steel bars. This methodology was applied by authors by writing MATLAB code and linking it with ABAQUS to determine the corresponding applied plastic load for each entered complementary strain energy. Generally, applying optimization problem for each model showed that the complementary strain energy of the residual forces reflects the general behaviour of the structures and may be assumed as a constraint controlling the plastic behaviour of the structures whereas the obtained results indicated how structures acted differently when possessing different complementary strain energy values turning from elastic into elasto-plastic condition and then reaching plastic state.

Keywords: optimal analysis; non-linear elasto-plastic analysis; complementary strain energy; reinforced concrete beam; reinforced concrete slab; limited residual plastic deformations

1 Introduction

Composite steel-concrete structures represent an efficient and economical form of construction for building and bridge applications leading to economical and efficient structural solutions. Therefore, steel behaviour is carried out in different cases and investigations [1, 2, 3, 4, 5]. On the other hand, controlling steel deformation is one of the most typical problems within metals processing where the

influence of residual stresses on fatigue behaviour is regarded as an essential issue to control the steel behaviour. Over the last few years, an increasing number of investigations have been held out to understand the effects of residual stresses and deformations on mechanical performance, Christidis et al., [6] proposed an efficient and simple method for specifying ultimate seismic displacements generated in steel frames caused by the residual deformation by investigating the non-elastic behaviour of various steel frames subjected to powerful ground movements. Therefore, based on comprehensive parametric investigations, observed equations are made to determine the seismic displacement that can be calculated after powerful seismic possibilities. And as a result, the usage of residual deformations could be effectively employed to estimate the performance status of steel structures after an earthquake. Generally, Residual stresses appear in numerous simulated structures and features so a large number of researches investigated this phenomenon. Gradually, various techniques have been created to calculate residual stress for diverse kinds of elements to get a dependable estimation. The different techniques have developed over many years and their applications have significantly aided by the growth of complementary methods like computing power and numerical methods. Rossini et al., [7] classified the various residual stresses measuring techniques and provided a summary of some recent advancements to assist investigators in choosing their methods between destructive, semi-destructive, and non-destructive methods depending on the application and the availabilities of the methods. Considering extensive parametric research on structures with a single degree of freedom structures, Hatzigeorgiou et al. [8], constructed practical formulas for an uncomplicated and adequate calculation of the maximum seismic deformation using residual displacements, that can be computed after powerful seismic events.

As for concrete, it is major to understand the behavior of this essential material, that is why, different researchers considered studying concrete properties experimentally and numerically [9, 10, 11]. The concrete damaged plasticity model (CDP) is presently one of the considerable concrete models employed for concrete simulation in ABAQUS. This model was described theoretically by Lubliner et al. in 1989 [12] then developed by Lee and Fenves in 1998 [13]. Where the model basically illustrates that there are two damage mechanisms including tensile cracking and compressive crushing of concrete, where the stiffness of the material is decreased by two damage parameters, individually for tension and compression, also the yield function is defined according to Lubliner [12] while the flow potential is a hyperbolic function [14]. Michał and Andrzej, [15] used the concrete damaged plasticity model (CDP) for modeling reinforced concrete structures using ABAQUS software. Performing numerical simulations concerning uniaxial and biaxial compression and uniaxial tension of a sample concrete specimen to be compared with experimental results. While, Shafieifar et al., [16] determined the tensile and compressive behaviour of ultra-high-performance concrete using the Concrete Damage Plasticity model (CDP) to define concrete performance in the absence of sufficient experimental data.

Plastic analysis and design methods are used when there are several engineering issues during the analysis and design of structures subjected to normal loads supplying details of the collapse and the post-yield behaviour benefiting in savings in materials. The optimal plastic design aims to make use of the plastic reserve of structures and to specify the optimal configuration of the material leading to a decrease in the overall weight or improving the load-carrying capacity. However, repeated plastic deformations and extreme residual displacements could be gathered and the structure might become unworkable. That is why limitations for the residual strains and displacements have to be involved in plastic analysis and design enabling the controlling of the plastic behaviour in structures.

As one of the oldest branches of mathematics, optimization theory catalyzed the development of geometry and differential calculus as it finds applications in a myriad of scientific and engineering disciplines [17, 18, 19]. Kaliszky and Logo, [20] presented three appropriate methods for the finding the optimal material form in the case of elasto-plastic structures under extreme loading. In meanwhile, Rohan and Whiteman [21] stated that the problem of optimal design belongs to a branch of the optimal control hypothesis that the control variable specifies the geometry of the issue aiming to find the shape of a compliant body so that an objective function reaches its minimum over an admissible set, where the general objective function affects both the state variables and the control variables as design parameters. As shape optimization for elastic deformation is easier than the elasto-plastic case, sensitivity analysis and optimization of elasto-plastic bodies are held as isotropic strain hardening takes place where the elasto-plastic behaviour of the material is controlled by a non-linear complementarity problem. Wang and Ohmori [22] utilized a cumulative elasto-plastic analysis approach forecasting the factor of the collapse load applied on a truss. The acquired factor of the collapse load is included in truss optimization used to develop the truss that keeps load-carrying capacity underneath standard load conditions and avoids collapse.

On the other hand, some applications of nonlinearity and concrete behavior were considered where Sae-Long et al. [23] suggested an efficient frame model with the inclusion of shear-flexure interaction for nonlinear analyses of columns normally presented in reinforced concrete (RC) frame buildings built prior to the introduction of modern seismic codes in the Seventies. While He et al. [24] considered the 3D printing procedure as a discontinuous control system and gave a straightforward and readable bond stress-slip model for a new and intelligent building 3-D printed concrete.

Besides, delivering a method for efficient prediction of areas in the structure as high stresses that lead to plastic deformation will occur. Where Strzalka et al. [25] proposed an investigation concentrated on the exploration of an efficient method for the a priori detection of a structural component's highly stressed areas. While an efficient method for the a priori detection of highly stressed areas of force-excited components was presented by Strzalka and Zehn [26], based on modal stress superposition. As the component's dynamic response and related stress are always

a function of its excitation, where certain attention is paid to the effect of the loading position.

This study aims to introduce a novel optimal elasto-plastic analysis method aiming to put the plastic behaviour of reinforced concrete structures under control by restraining the residual plastic deformations initating inside the steel bars of two selected models, a reinforced concrete beam [27] and a reinforced concrete slab [28], employing complementary strain energy of residual forces which is considered globally displacement limitation. Thereafter, these chosen structures were numerically calibrated using ABAQUS and CDP model [14], which defines the concrete damage developed in the structures. The used method is extended from the work originally produced by Kaliszky and Lógó [29]. Generally, the work in this study includes considering an objective function to optimize the applied plastic load assuming that the complementary strain energy is a constraint controlling the plastic behaviour of steel bars. Then, the authors created a non-linear optimization programming code using MATLAB and this was connected to the numerical models calibrated in ABAQUS where residual stresses were calculated after running the code for each increment in order to achieve the optimal load values, after that, the complementary strain energy was calculated and a comparison with the allowed value set in the MATLAB code was considered to investigate the influence of the complementary strain energy on the plastic limit of structures loading bearing capacity.

The structure of this paper includes the numerical modelling procedure of the two benchmarks in Section 2, while Section 3 has a clear description of the limited residual plastic deformation approach applied on steel bars. furthermore, Section 4 contains the formulations of the optimization problem, while Section 5 presents a summary of results and explanations of the optimized structures. Eventually, conclusions are demonstrated in Section 6.

2 Numerical Calibration of the Structures

2.1 Simple Reinforced Concrete Beam Case

Simply supported reinforced concrete beam model having concrete strength of 25 MPa was considered in this section [27]. The test programs consisted of manufacturing and testing RC beam with rectangular cross-section of 250 mm x 350 mm and a length of 2500 mm, under four-point load as displayed in Fig. 1 where the details of the chosen model S20-1 are clarified. Sequentially, this beam was calibrated by ABAQUS as indicated in Fig. 2 using the CDP model to define concrete behavior where a 3D eight nodes solid element (C3D8) was used to represent concrete, while the reinforcement bars were represented as a 3D beam element with a 2-node linear beam in space (B31). Consequently, crack patterns and

load-deflection curves were acquired as illustrated in Figs. 3 and 4, which clearly show that the numerical results are agreeing with the experimental results given by the study.

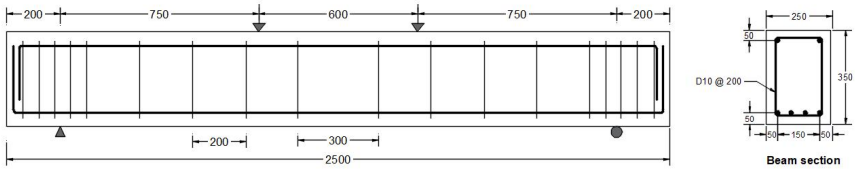

Figure 1
Details of S20-1 model

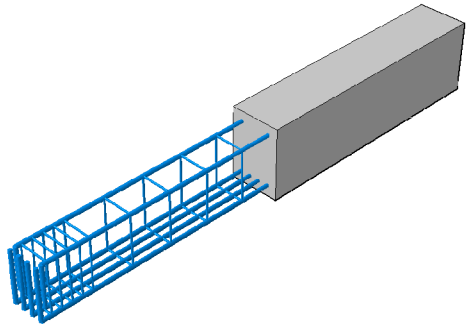

Figure 2
S20-1 numerical modelling

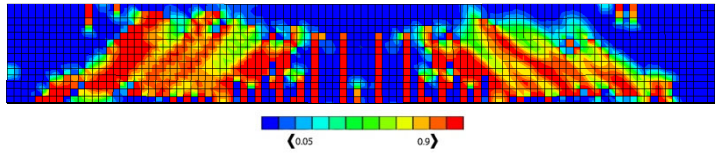

Figure 3
Crack patterns of S20-1 model

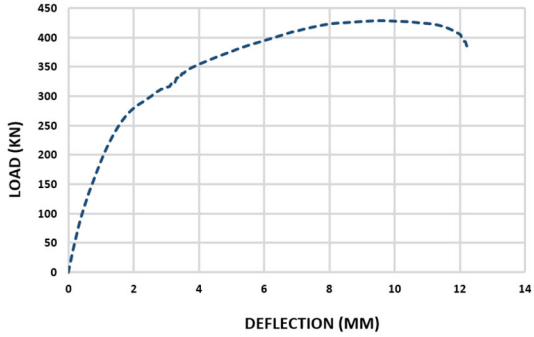

Figure 4
Load-Deflection relationship for S20-1 model

2.2 Reinforced Concrete Slab Case

In this section, a one-way reinforced concrete slab model (SP1) was considered [28] with 1750 mm in length, 700 mm in width, and 100 mm in depth. The slab was tested under two-point load with 500 mm load distance, and supported with a clear span of 1725 mm, also, the reinforcement bars were 8 mm in diameter. Fig. 5 shows the model properties where this model was calibrated using ABAQUS by applying a 3D eight nodes solid element (C3D8) to represent the concrete, while as the reinforcement bars were represented as a 3D beam element with a 2-node linear beam in space (B31) as shown in Fig. 6. As a result, crack patterns and load-deflection curves were obtained for the slab as displayed in Figs. 7 and 8, and these results are compatible with the experimental results offered by the study.

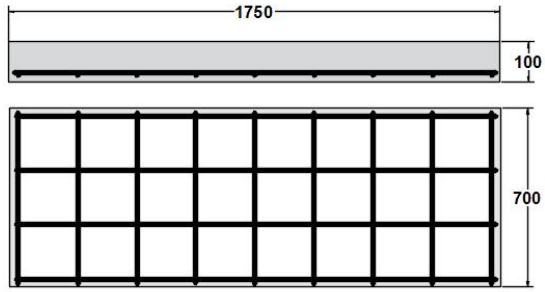

Figure 5
Details of SP1 model

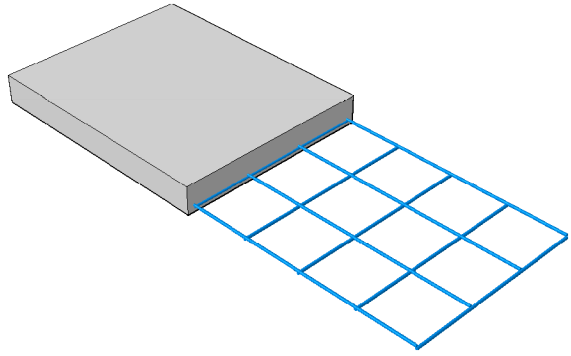

Figure 6
Numerical modelling of SP1

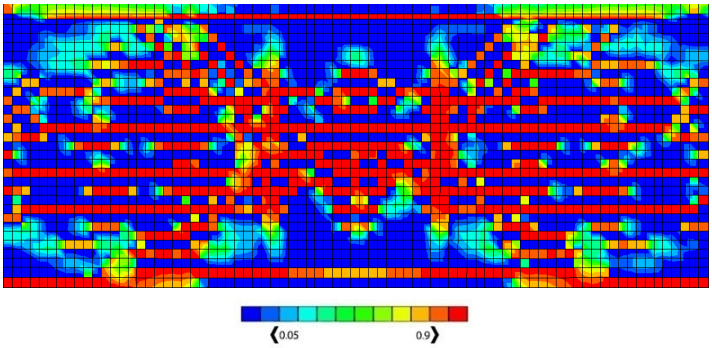

Figure 7
Crack patterns for SP1 model

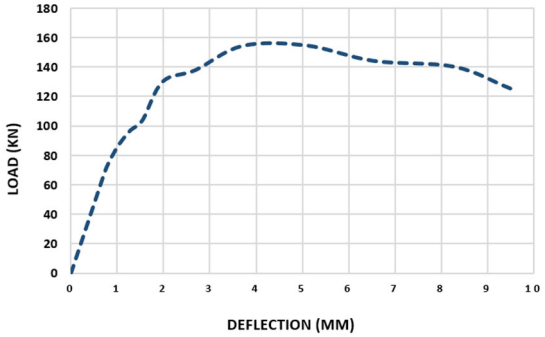

Figure 8
Load-Deflection relationship for SP1 model

3 Limited Residual Plastic Deformation Theory Applied on Steel Bars

Presenting the Euler notation, assume a body formed of elasto-plastic, time- and temperature-independent material with volume V and surface S. A part of S, S_u is under zero surface displacements, whilst the remaining part S_q, is under quasi-static surface tractions $q_i\,(t)$. The subsequent amounts regarding the surface tractions $q_i\,(t)$ are described at time t, as [30, 31]:

$\sigma_{ij}(t)$ = actual stresses,

$\epsilon_{ij}(t)$ and $u_i(t)$ = actual strains and displacements,

$\sigma_{ij}^{el}(t)$ = fictitious stresses that would occur if the material were purely elastic,

$\epsilon_{ij}^{el}(t)$ and $u_i^{el}(t)$ = fictitious elastic strains and displacements corresponding to $\sigma_{ij}^{el}(t)$, besides, the following different self-stress distributions are introduced:

$\sigma_{ij}^{R}(t)$ = actual residual stress distribution,

$\bar{\sigma}_{ij}^{R}$ = any arbitrary, time-independent self-stress distribution.

The real strain is divided into elastic and plastic parts, as shown in Eq. (1). Devoting the latest notation, the elastic strain parts are linked to real stresses by the constitutive law,

$$\epsilon_{ij} = \epsilon_{ij}^{el} + \epsilon_{ij}^{pl} \tag{1}$$

$$\epsilon_{ij}^{el} = C_{ijkl}\sigma_{kl}^{el} \tag{2}$$

As the plastic strain ϵ_{ij}^{pl} and the elastic tensor C_{ijkl} are expressed by the accompanied flow rule,

$$\epsilon_{ij}^{pl} = \lambda \frac{\partial f}{\partial \sigma_{ij}}, \quad \lambda \geq 0 \text{ if } f = 0 \text{ and } \dot{f} = 0, \quad \text{otherwise } \lambda = 0 \tag{3}$$

here $f(\sigma_{ij})$ is the yield function and $f(\sigma_{ij}) = 0$ defines a convex surface in the stress space.

Yet, the fictitious elastic stresses $\sigma_{ij}^{el}(t)$, the actual stresses $\sigma_{ij}(t)$, and the actual residual stresses σ_{ij}^{R} should fulfill the next relation:

$$\sigma_{ij}(t) = \sigma_{ij}^{el}(t) + \sigma_{ij}^{R} \tag{4}$$

here $\sigma_{ij}^{el}(t)$ is related to the fictitious elastic strain $\epsilon_{ij}^{el}(t)$ by the constitutive law,

$$\epsilon_{ij}^{el}(t) = C_{ijkl}\sigma_{kl}^{el}(t). \tag{5}$$

Assume the entire complementary plastic work $W_p(\tau)$ achieved during a load path from the undisturbed state at $t = 0$ up to $t = \tau$. This outcome could be regarded as an appropriate measurement in evaluating the plastic behaviour and general plastic deformation of an elasto-plastic body. Its upper bound can be acquired by the subsequent theory presented by Capurso [32, 33] and Capurso et al. [34, 35].

If any time-independent distribution of self-stresses $\bar{\sigma}_{ij}^{R}$ could be discovered so that the situation:

$$f\left(\sigma_{ij}^{E}(t) + \bar{\sigma}_{ij}^{R}\right) \leq 0 \tag{6}$$

is satisfied in V at any time $t \leq \tau$, then the total complementary plastic work is upper bounded by the condition:

$$W_p(\tau) \leq \frac{1}{2}\int C_{ijkl}\ \bar{\sigma}_{ij}^{R}\ \bar{\sigma}_{kl}^{R}\ dV. \tag{7}$$

It can be seen that the bound may be enhanced using the proper selection of ($\bar{\sigma}_{ij}^{R}$) [32, 33]. Considering the bound on the complementary plastic work illustrated by Eq. (7). To stop excessive plastic deformations, set a suitably selected allowed W_{p0} on the plastic work W_p. The boundaries of the plastic deformations are defined by the existent residual stresses; i.e., it is assumed that:

$$\bar{\sigma}_{ij}^{R} \equiv \sigma_{ij}^{R}. \tag{8}$$

This assumption delivers a reasonable upper bound and permits a proper form of the issue. Thus, the plastic deformation constraint will be:

$$W_p(\tau) = \frac{1}{2}\int_V C_{ijkl}\,\sigma_{ij}^{R}\,\sigma_{kl}^{R} dV - W_{p0} \leq 0. \tag{9}$$

Consequently, a proper computational approach was suggested that the complementary strain energy of the residual forces may be described as a general measure of the plastic behaviour of structures whereas the residual deformations are needed to be restrained using boundaries for such energy amount. Eq. (9) were created regarding the case of bar elements, the complementary strain energy is calculated by the residual forces as the following:

$$W_p = \frac{1}{2\mathrm{E}} \sum_{\mathrm{i}=1}^{\mathrm{n}} \frac{\mathrm{l_i}}{A_i} N_i^{R^2} \leq W_{p0} \tag{10}$$

where W_{p0} is a suitable permissible energy value for W_p and can be derived from the elastic strain energy of the structure (see, e.g., Kaliszky and Lógó [36]). Also, $l_i, (i = 1, 2, \dots, n)$ represents the length of the member (bar elements), while the area of bar elements cross-section is represented by, $A_i, (i = 1, 2, \dots, n)$ while N_i^R denotes the residual force of the bar members and E is Young's modulus of the material of bars. By applying Eq. (10), the plastic deformations of bar elements are limited as a suitable limited value W_{p0} is presented.

Besides, the residual forces N^R that held in the structure after finishing the unloading are introduced by the internal plastic force N^{pl} which will occur in the structure by applying the loading P_0 and the elastic internal force$-N^{el}$:

$$N^R = N^{pl} - N^{el} \tag{11}$$

where:

$$N^{el} = F^{-1} G^T K^{-1} P_0 \tag{12}$$

Where the flexibility matrix is represented by F; whilst the geometrical matrix is denoted by G; moreover, the stiffness matrix is represented by K. Mainly, this approach will be used on the steel bars used to reinforce the RC structures for controlling the plastic deformation developed within, nevertheless, the internal forces generated in the concrete are not counted during the optimization problem because of its weak contribution in tension if compared with steel.

4 Optimization Problem

The mathematical equation to determine the optimal load value of RC structures is arranged in this part. A non-linear optimization approach is proposed to obtain the maximum optimal plastic load (F^{pl}) applied to the selected models, employing the extremum plasticity principles, the step-by-step redeveloped constitutive elements are not needed. The next equations represent the elements employed in the optimization code where the purpose is to maximize the applied load (F^{pl}) whilst the plastic deformation is controlled (W_{p0} value) using the constraints provided, also, A_i and l_i describe the cross-section area and length of each steel element, respectively.

$$Max. \rightarrow F^{pl} \tag{13a}$$

$$Subjected\ to:\ N^{el} = F^{-1}GK^{-1}P_0; \tag{13b}$$

$$-\overline{N^{pl}} \leq N^{Pl} \leq \overline{N^{pl}}; \tag{13c}$$

$$\frac{1}{2\mathrm{E}} \sum_{\mathrm{i}=1}^{\mathrm{n}} \frac{\mathrm{l_i}}{A_i} N_i^{R^2} \leq W_{p0}. \tag{13d}$$

Eq. (13b) shows the estimation of the elastic fictitious internal normal forces developed in the steel elements, whilst the inequality Eq. (13c) indicates the lower- and upper-plastic limit conditions, whereas $\overline{N^{pl}}$ represents the ultimate plastic limit load. Furthermore, boundary Eq. (13d) shows the complementary strain energy of residual forces employed for controlling the plastic deformations in steel elements as a globally known measurement of plastic behaviour of the structures. Fig. 9 describes the procedure of the optimization problem as the CDP parameters used in the optimization problem are regarded constants.

Essentially, the boundary of plastic deformation employing complementary strain energy is used on steel bars located inside RC structures for controlling the plastic deformation developed within. However, the internal forces developed in the concrete are not included during the optimization process due to its weak contribution in tension in comparison with steel where it is comprehended that tension strain in steel is higher than tension strain in concrete that can drive the early collapse of concrete subjected to tension condition.

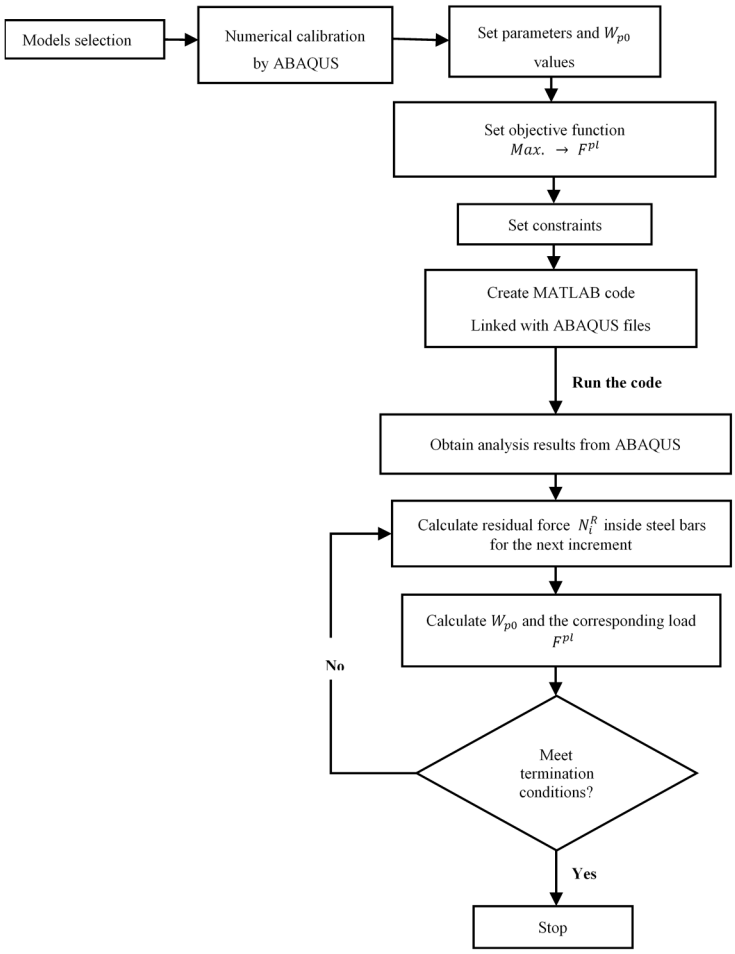

Figure 9
Optimization problem process

5 Results and Discussions

5.1 Simple Reinforced Concrete Beam Case

In this part, the results of having reinforced concrete beam are presented and discussed. Apparently, Fig. 10 displays the load-$\boldsymbol{W_{p0}}$ relationship for S20-1 beam noting that as $\boldsymbol{W_{p0}}$ value increases, the related load is increasing too showing a higher plasticity condition. When $\boldsymbol{W_{p0}}$ value is zero, the curve is within an elastic

state, nevertheless, the curve starts pushing towards the plastic state when $\boldsymbol{W_{p0}}$ value increases.

Additionally, Table 1 demonstrates steel stress intensity for the model assuming different cases of $\boldsymbol{W_{p0}}$, and it is clear that the red spots that symbolize high-stress intensity in steel are increasing as $\boldsymbol{W_{p0}}$value increases as the colour varies from blue (low-stress intensity in steel) into red (high-stress intensity in steel). Eventually, having such results proves the effectiveness of the complementary strain energy as a plasticity controller that makes it possible in expecting and controlling the plastic failure behaviour of the beam.

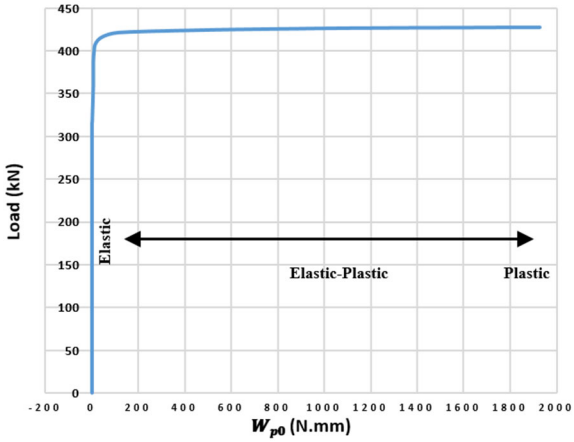

Figure 10
Load-$\boldsymbol{W_{p0}}$ relationship for S20-1 model

Table 1
$Wp0$ - load effect on the stress intensity of S20-1 model

$\boldsymbol{W_{p0}}$ (N.mm)	P (kN)	Stress intensity
0	*300*	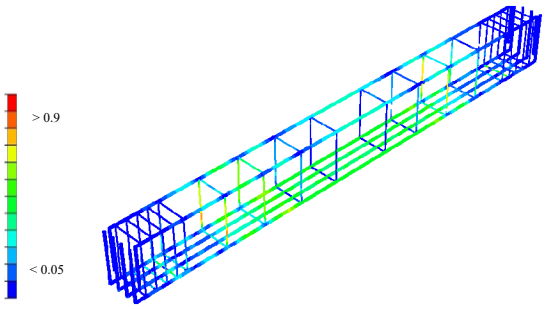

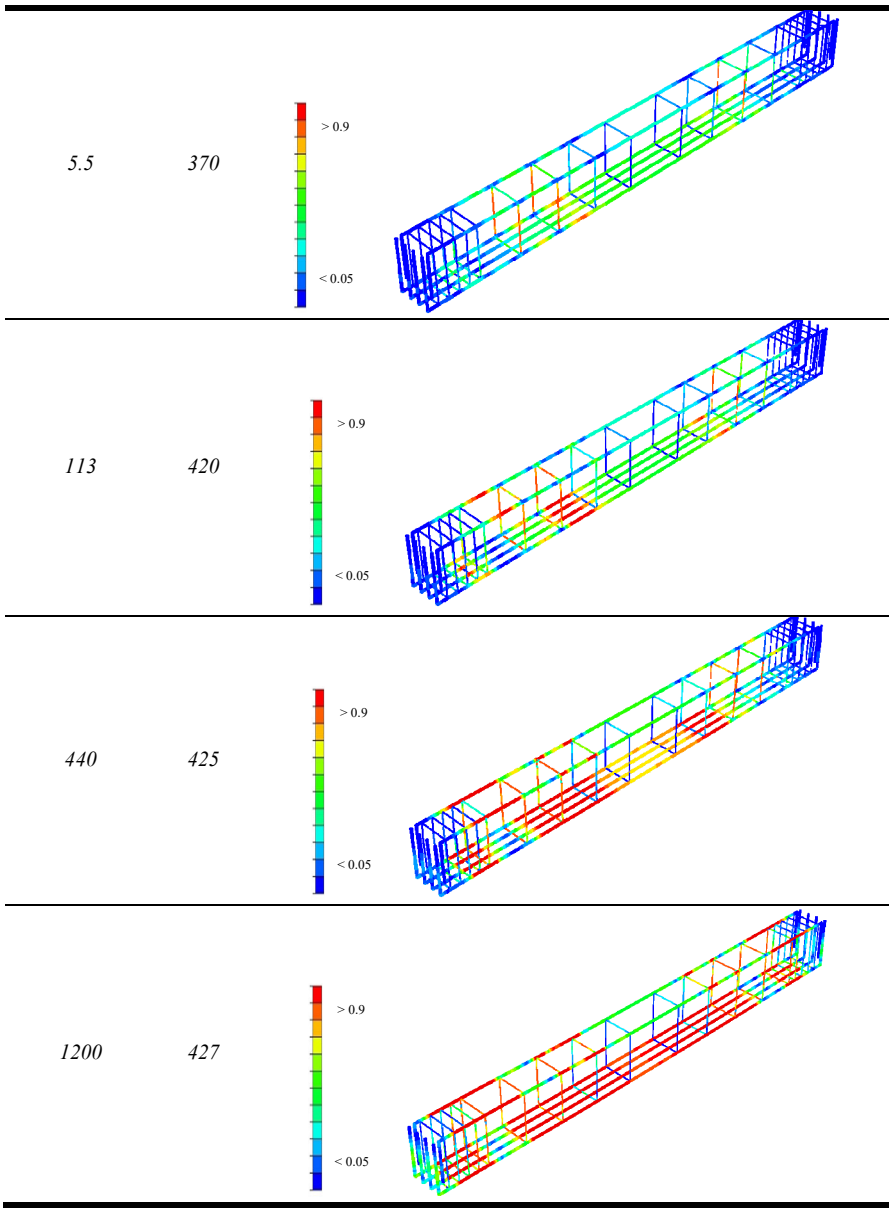

5.2 Reinforced Concrete Slab Case

The results of having reinforced concrete slab are illustrated and discussed in this section where it is worth mentioning that the bars in the long direction are not yielded in this case as the slab is working as a one-way slab. Apparently, Fig. 11 shows the load-$\boldsymbol{W_{p0}}$ relationship for the selected slab noting that by the increment

of $\boldsymbol{W_{p0}}$ value, the corresponding load is increasing too indicating that higher plasticity state is acquired that when $\boldsymbol{W_{p0}}$ value is zero, the curve act in elastic condition, yet, the curve begins proceeding towards plastic state as $\boldsymbol{W_{p0}}$ value growths.

For more explanations, Table 2 displays steel stress intensity for SP1 model considering various possibilities of $\boldsymbol{W_{p0}}$, and by comparison, it is detected that the red spots that shows high-stress intensity in steel, increase when $\boldsymbol{W_{p0}}$ value increases as the colour goes from blue (low-stress intensity in steel) into red (high-stress intensity in steel). So, having such outcomes proves the usefulness of the complementary strain energy as a plasticity controller which makes it likely in predicting and controlling the plastic failure behaviour of the slab.

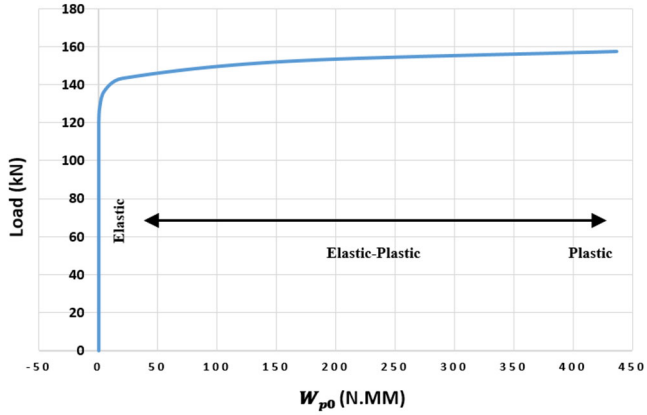

Figure 11
Load-$\boldsymbol{W_{p0}}$ relationship for SP1 model

Table 2
$Wp0$ - load effect on the stress intensity of SP1 model

$\boldsymbol{W_{p0}}$ (N.mm)	P (kN)	Stress intensity
0	*70*	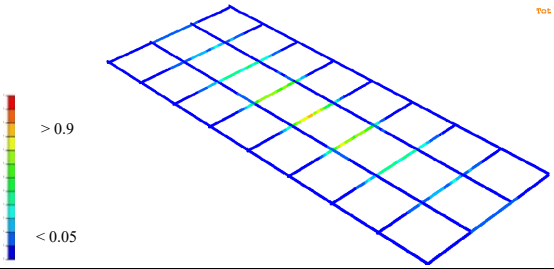

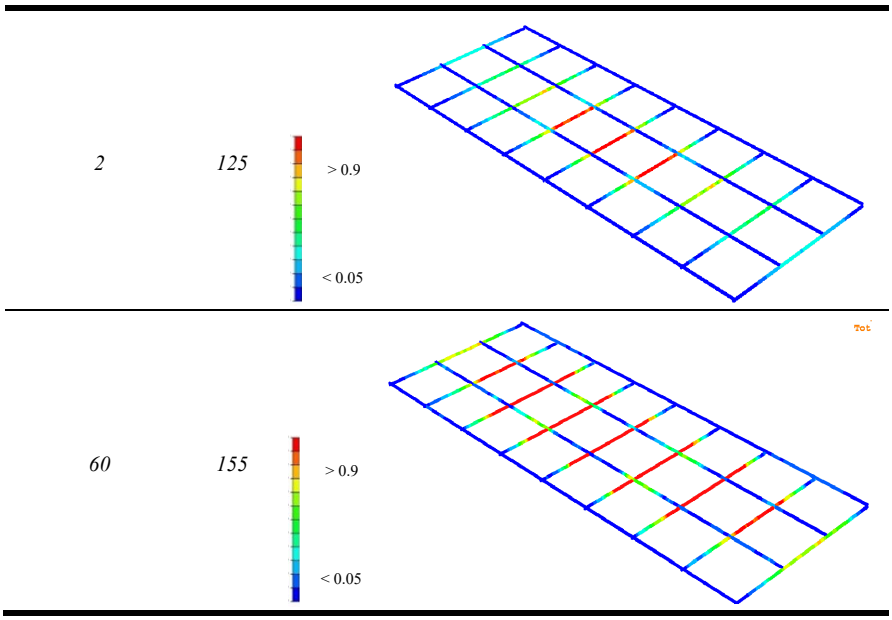

Conclusions

In this investigation, the optimal analysis problem of RC structures was studied. Thus, a numerical calibration process was carried out in order to validate the two benchmarks selected from earlier studies [27, 28] where the concrete damage plasticity (CDP) constitutive model was employed to define the behaviour of the used concrete. Sequentially, an optimization problem was used to maximize the plastic loading while controlling the plastic deformations by employing the complementary strain energy of the residual internal forces $\boldsymbol{W_{p0}}$ as a constraint. Eventually, different points were concluded whereas $\boldsymbol{W_{p0}}$ value increases, the corresponding load is increasing too indicating that a higher plasticity state is acquired. Moreover, when $\boldsymbol{W_{p0}}$ value is small, the curves are within elastic region, nonetheless, the curves start moving towards plastic region as $\boldsymbol{W_{p0}}$ value increases.

References

[1] Kurhan, D., Kurhan, M. and Husak, M., 2020, November. Impact of the variable stiffness section on the conditions of track and rolling stock interaction. In IOP Conference Series: Materials Science and Engineering (Vol. 985, No. 1, p. 012005) IOP Publishing

[2] Kurhan, M., Kurhan, D., Novik, R., Baydak, S. and Hmelevska, N., 2020, November. Improvement of the railway track efficiency by minimizing the rail wear in curves. In IOP Conference Series: Materials Science and Engineering (Vol. 985, No. 1, p. 012001) IOP Publishing

[3] Mahmood, T., Haleemzai, I., Ali, Z., Pamucar, D. and Marinkovic, D., 2022. Power Muirhead Mean Operators for Interval-Valued Linear Diophantine Fuzzy Sets and Their Application in Decision-Making Strategies. Mathematics, 10(1), p.70

[4] Kuchak, A. J. T., Marinkovic, D. and Zehn, M., 2021. Parametric investigation of a rail damper design based on a lab-scaled model. Journal of Vibration Engineering & Technologies, 9(1), pp. 51-60

[5] Németh, A. and Fischer, S., 2021. Investigation of the glued insulated rail joints applied to CWR tracks. Facta Universitatis, Series: Mechanical Engineering, 19(4), pp. 681-704, https://doi.org/10.22190/FUME210331040N

[6] Christidis, A. A., Dimitroudi, E. G., Hatzigeorgiou, G. D. and Beskos, D. E., 2013. Maximum seismic displacements evaluation of steel frames from their post-earthquake residual deformation. Bulletin of Earthquake Engineering, 11(6), pp. 2233-2248, https://doi.org/10.1007/s10518-013-9490-z

[7] Rossini, N. S., Dassisti, M., Benyounis, K. Y. and Olabi, A. G., 2012. Methods of measuring residual stresses in components. Materials & Design, 35, pp. 572-588, https://doi.org/10.1016/j.matdes.2011.08.022

[8] Hatzigeorgiou, G. D., Papagiannopoulos, G. A. and Beskos, D. E., 2011. Evaluation of maximum seismic displacements of SDOF systems from their residual deformation. Engineering structures, 33(12), pp. 3422-3431, https://doi.org/10.1016/j.engstruct.2011.07.006

[9] Saberi Varzaneh, A. and Naderi, M., 2020. Experimental and Finite Element Study to Determine the Mechanical Properties and Bond Between Repair Mortars and Concrete Substrates. Journal of Applied and Computational Mechanics

[10] Di Re, P. and Addessi, D., 2021. Computational Enhancement of a Mixed 3D Beam Finite Element with Warping and Damage. Journal of Applied and Computational Mechanics

[11] He, C. H., Liu, C., He, J. H., Mohammad-Sedighi, H., Shokri, A. and Gepreel, K. A., 2021. A fractal model for the internal temperature response of a porous concrete. Appl. Comput. Math, 20(2)

[12] Lubliner, J., Oliver, J., Oller, S. and Oñate, E., 1989. A plastic-damage model for concrete. International Journal of solids and structures, 25(3), pp. 299-326, https://doi.org/10.1016/0020-7683(89)90050-4

[13] Lee, J. and Fenves, G. L., 1998. Plastic-damage model for cyclic loading of concrete structures. Journal of engineering mechanics, 124(8), pp. 892-900, https://doi.org/10.1061/(ASCE)0733-9399(1998)124:8(892)

[14] Abaqus/CAE ver. 6-12.2, Dassault Systemes Simulia Corp., 2012

[15] Michał, S. and Andrzej, W., 2015. Calibration of the CDP model parameters in Abaqus. World Congr. Adv. Struct. Eng. Mech.(ASEM 15), Incheon Korea

[16] Shafieifar, M., Farzad, M. and Azizinamini, A., 2017. Experimental and numerical study on mechanical properties of Ultra High Performance Concrete (UHPC). Construction and Building Materials, 156, pp. 402-411, https://doi.org/10.1016/j.conbuildmat.2017.08.170

[17] Tauzowski, P., Blachowski, B. and Lógó, J., 2021. Topology optimization of elasto-plastic structures under reliability constraints: A first order approach. Computers & Structures, 243, p. 106406, https://doi.org/10.1016/j.compstruc.2020.106406

[18] Błachowski, B., Świercz, A., Ostrowski, M., Tauzowski, P., Olaszek, P. and Jankowski, Ł., 2020. Convex relaxation for efficient sensor layout optimization in large ‐ scale structures subjected to moving loads. Computer ‐ Aided Civil and Infrastructure Engineering, 35(10), pp. 1085-1100, https://doi.org/10.1111/mice.12553

[19] Blachowski, B., Tauzowski, P. and Lógó, J., 2020. Yield limited optimal topology design of elastoplastic structures. Structural and Multidisciplinary Optimization, 61(5), pp. 1953-1976, https://doi.org/10.1007/s00158-019-02447-9

[20] Kaliszky, S. and Logo, J., 2006. Optimal design of elasto-plastic structures subjected to normal and extreme loads. Computers & structures, 84(28), pp. 1770-1779, https://doi.org/10.1016/j.compstruc.2006.04.009

[21] Rohan, E. and Whiteman, J. R., 2000. Shape optimization of elasto-plastic structures and continua. Computer Methods in Applied Mechanics and Engineering, 187(1-2), pp. 261-288, https://doi.org/10.1016/S0045-7825(99)00134-6

[22] Holzer, S. M. and Yosibash, Z., 1996. The p ‐ version of the finite element method in incremental elasto ‐ plastic analysis. International journal for numerical methods in engineering, 39(11), pp. 1859-1878, https://doi.org/10.1002/(SICI)1097-0207(19960615)39:11<1859::AID-NME932>3.0.CO;2-7

[23] Sae-Long, W., Limkatanyu, S., Hansapinyo, C., Imjai, T. and Kwon, M., 2020. Forced-based shear-flexure-interaction frame element for nonlinear analysis of non-ductile reinforced concrete columns. Journal of Applied and Computational Mechanics. doi: 10.22055/jacm.2020.32731.2065

[24] He, C. H., Liu, S. H., Liu, C. and Mohammad-Sedighi, H., 2021. A novel bond stress-slip model for 3-D printed concretes. Discrete & Continuous Dynamical Systems-S. doi: 10.3934/dcdss.2021161

[25] Strzalka, C., Marinkovic, D. and Zehn, M. W., 2021. Stress mode superposition for a priori detection of highly stressed areas: Mode normalisation and loading influence

[26] Strzalka, C. and Zehn, M., 2020. The influence of loading position in a priori high stress detection using mode superposition. Reports in Mechanical Engineering, 1(1), pp. 93-102, https://doi.org/10.31181/rme200101093s

[27] Lee, J. Y., Choi, I. J. and Kim, S. W., 2011. Shear Behavior of Reinforced Concrete Beams with High-Strength Stirrups. ACI Structural Journal, 108(5)

[28] Adam, M. A., Erfan, A. M., Habib, F. A. and El-Sayed, T. A., 2021. Structural Behavior of High-Strength Concrete Slabs Reinforced with GFRP Bars. Polymers, 13(17), p. 2997, https://doi.org/10.3390/polym13172997

[29] Kaliszky, S. and Lógó, J., 1995. Elasto-plastic analysis and optimal design with limited plastic deformations and displacements. In: Structural and Multidisciplinary Optimization, ed. by N. Olhoff, G. I. N. Rozvany, Pergamon Press, 465-470

[30] Rahmanian, I., Lucet, Y. and Tesfamariam, S., 2014. Optimal design of reinforced concrete beams: A review. Computers and Concrete, 13(4), pp. 457-482

[31] Kaliszky S. Elastoplastic analysis with limited plastic deformations and displacements. Journal of Structural Mechanics. 1996, 24(1):39-50, https://doi.org/10.1080/08905459608905254

[32] Capurso M. A displacement bounding principle in shakedown of structures subjected to cyclic loads. International Journal of Solids and Structures. 1974, 10(1):77-92, https://doi.org/10.1016/0020-7683(74)90102-4

[33] Chutani, S. and Singh, J., 2017. Design optimization of reinforced concrete beams. Journal of The Institution of Engineers (India): Series A, 98(4), pp. 429-435

[34] Capurso M, Corradi L, Maier G. Bounds on deformations and displacements in shakedown theory. Proc. Materiaux et Structures sous Chargement Cyclique. Palaiseau. ass. amicale des ingénieursanciens eléves de l'E.N.P.C., Paris, France. 1978, 231-244

[35] Tin-Loi F. Optimum shakedown design under residual displacement constraints. Structural and Multidisciplinary Optimization. 2000, 19(2):130-139, https://doi.org/10.1007/s001580050093

[36] Kaliszky S, Lógó J. Optimal plastic limit and shake-down design of bar structures with constraints on plastic deformation. Engineering Structures. 1997, 19(1):19-27